

SPECT/CT Imaging of the Novel HER2-Targeted Peptide Probe ^{99m}Tc -HYNIC-H6F in Breast Cancer Mouse Models

Liqiang Li^{*1}, Yue Wu^{*1}, Zihua Wang², Bing Jia^{1,3}, Zhiyuan Hu², Chengyan Dong^{†4}, and Fan Wang^{†1,4}

¹Medical Isotopes Research Center and Department of Radiation Medicine, School of Basic Medical Sciences, Peking University, Beijing, China; ²CAS Key Laboratory for Biomedical Effects of Nanomaterials and Nanosafety, National Center for Nanoscience and Technology of China, Beijing, China; ³Medical and Healthy Analytical Center, Peking University, Beijing, China; and ⁴Key Laboratory of Protein and Peptide Pharmaceuticals, CAS Center for Excellence in Biomacromolecules, Institute of Biophysics, Chinese Academy of Sciences, Beijing, China

Overexpression of human epidermal growth factor receptor 2 (HER2) plays important roles in tumorigenesis and tumor progression in breast cancer. Nuclear imaging of HER2 expression in tumors might detect all HER2-positive tumors throughout the body and guide HER2-targeted therapies for patients. We therefore aimed to develop a HER2-targeted peptide probe for breast cancer imaging. A novel SPECT imaging probe, ^{99m}Tc -HYNIC-H6F, was prepared and then evaluated in breast cancer animal models. **Methods:** The HER2-targeted peptide H6F (YLFFVFER) was conjugated with the bifunctional chelator hydrazinonicotinamide (HYNIC). ^{99m}Tc -HYNIC-H6F was prepared, and the in vivo characteristics of ^{99m}Tc -HYNIC-H6F were investigated in MDA-MB-453 (HER2-positive) and MDA-MB-231 (HER2-negative) models using small-animal SPECT/CT. Moreover, to investigate the specificity of the H6F peptide toward HER2 and the potential applications in monitoring therapies involving trastuzumab, unlabeled H6F and trastuzumab were used as blocking agents in cell competition studies and SPECT imaging. **Results:** A standard tricine/trisodium triphenylphosphine-3,3',3''-trisulfonate labeling procedure demonstrated that the radiochemical purity was greater than 95%. ^{99m}Tc -HYNIC-H6F displayed excellent HER2-binding specificity both in vitro and in vivo. SPECT/CT imaging revealed that the MDA-MB-453 tumors were clearly visualized (percentage injected dose per gram, 3.58 ± 0.01 at 30 min after injection), whereas the signals in HER2-negative MDA-MB-231 tumors were much lower (0.73 ± 0.22 at 30 min after injection). Tumor uptake of MDA-MB-453 was blocked by the coinjection of excess H6F but not by excess trastuzumab. **Conclusion:** The ^{99m}Tc -HYNIC-H6F peptide probe specifically accumulates in HER2-positive tumors and is therefore promising for the diagnosis of HER2-positive cancers. Because ^{99m}Tc -HYNIC-H6F and trastuzumab target different regions of the HER2 receptor, this radiotracer also has great potential for monitoring the therapeutic efficacy of trastuzumab by rechecking the expression level of HER2 without blocking effect during therapy.

Key Words: HER2; breast cancer; SPECT; targeting peptide; trastuzumab

J Nucl Med 2017; 58:821–826

DOI: 10.2967/jnumed.116.183863

Breast cancer is the most frequent cancer and the second leading cause of cancer death among women worldwide. The great progress in breast cancer screening and early diagnosis in recent decades has significantly increased life expectancy and patient quality of life (1,2). The best-studied tumor-associated antigen in breast cancer is human epidermal growth factor receptor 2 (HER2), which is positive in approximately 20%–30% of all breast cancers (3–5). Moreover, overexpression of HER2 is also characterized as a major negative prognostic factor that is associated with higher mortality in early-stage disease, increased incidence of metastasis, and reduced time to relapse (6–8). Trastuzumab (Herceptin; Genentech), the first approved HER2-targeted humanized monoclonal antibody, is the standard-of-care treatment for patients with HER2-positive breast cancer. In several trials, trastuzumab has proven effective in combination with or after standard chemotherapy (9–11). HER2 expression status in histopathologic samples of primary cancer or metastatic tissue can be analyzed by immunohistochemistry or fluorescence in situ hybridization in clinical practice (12). However, biopsy is invasive, and tumor heterogeneity can lead to variable results (13). Intermetastatic, intrametastatic and even intratumoral heterogeneity in breast cancers also make indirect approaches such as serum HER2 immunoassays insufficient to predict long-term responses or to appropriately change the treatment schedule. Thus, a more accurate and noninvasive method to assess the HER2 expression of whole-body tumors is needed (14).

Nuclear imaging may represent an appropriate tool to obtain real-time and quantifiable information about HER2 expression with high sensitivity and spatial resolution and remedy current deficiencies in the assessment of HER2 expression in vivo (15). In several preclinical and clinical studies, radiolabeled trastuzumab and pertuzumab have shown high accumulation in tumor tissues (16,17). But the best time for assessment of antibody-based imaging with reasonable tumor-to-organ ratios is typically 3–5 d after administration, which may delay the treatment modification. Thus, small-molecule alternatives such as ScFv-Fc, F(ab')₂, minibody, diabody, and Affibody molecules were developed and radiolabeled as cancer diagnosis probes (18). The decreased molecular size of these molecules alters the clearance pathway to enable favorable imaging properties. As small targeting molecules, peptides exhibit relatively short circulatory half-lives, good penetration, low immunogenicity, and ease of chemical modification and are thus more suitable for clinical imaging procedures (19,20). Although

Received Sep. 8, 2016; revision accepted Dec. 20, 2016.

For correspondence or reprints contact: Fan Wang, Medical Isotopes Research Center, Peking University, 38 Xueyuan Rd., Beijing 100191, P. R. China.

E-mail: wangfan@bjmu.edu.cn

*Contributed equally to this work.

†Contributed equally to this work.

Published online Jan. 19, 2017.

COPYRIGHT © 2017 by the Society of Nuclear Medicine and Molecular Imaging.

numerous peptide-based imaging agents have been synthesized and translated from bench to bed (21), HER2-targeted peptides for nuclear imaging remain underdeveloped.

We previously screened out a novel HER2-targeted peptide, H6F (YLFFVFER), using a one-bead one-compound combinatorial library approach. In vivo and ex vivo experiments demonstrated that the H6F peptide has high affinity and high specificity toward HER2 (22). In the present study, we developed this H6F peptide as a SPECT imaging probe for in vivo breast cancer HER2 detection and evaluated its targeting capability in subcutaneous human breast cancer xenografts.

MATERIALS AND METHODS

Cell Culture and Animal Models

The MDA-MB-453 and MDA-MB-231 human breast cancer cell lines were obtained from China Infrastructure of Cell Line Resources and were grown in Leibovitz L-15 medium. Both cell lines were cultured in medium supplemented with 10% fetal bovine serum at 37°C in a humidified atmosphere containing 5% CO₂.

All animal experiments were performed in accordance with the guidelines of the Peking University Animal Care and Use Committee. To obtain MDA-MB-453 and MDA-MB-231 subcutaneous tumor models, MDA-MB-453 cells (1×10^7 in 200 μ L of phosphate-buffered saline) or MDA-MB-231 cells (6×10^6 in 200 μ L of phosphate-buffered saline) were inoculated subcutaneously into the right front flanks of female BALB/c nude mice. The animals were used for in vivo studies when the tumor size reached 100–150 mm³ (2–3 wk after inoculation).

Preparation of ^{99m}Tc-Hydrazinonicotinamide (HYNIC)-H6F

The H6F peptide and fluorescein isothiocyanate (FITC)-H6F were synthesized as previously described (22). The H6F peptide was then conjugated with SBz-HYNIC using a standard procedure (23). A solution of 2 μ mol of H6F peptide was mixed with 6 μ mol of SBz-HYNIC in 500 μ L of dimethylformamide. After stirring of the solution at room temperature for 6 h, HYNIC-H6F was isolated by semipreparative high-performance liquid chromatography (HPLC) and lyophilized to afford the final product. HYNIC-H6F was labeled with ^{99m}Tc using tricine and tricine/trisodium triphenylphosphine-3,3',3''-trisulfonate as the coligands (23) and then purified with Sep-Pak C18 cartridges (Waters). After purification, the radiochemical purity of ^{99m}Tc-HYNIC-H6F was determined by radio-HPLC.

Fluorescence Staining and Flow Cytometry

To evaluate the expression status of HER2 in different breast cancer cells, fluorescence staining and flow cytometry of MDA-MB-453 and MDA-MB-231 cells were performed. In the cell-staining experiment, approximately 1×10^5 MDA-MB-453 and MDA-MB-231 breast cancer cells in 1 mL of medium were seeded into culture dishes and incubated with FITC-trastuzumab solution (200 μ g) and Hoechst 33342 (1 mmol/L) for 120 min at 4°C and visualized using a confocal microscope (Wetzler). In the flow cytometry experiment, the cells were harvested and suspended in phosphate-buffered saline supplemented with 1% bovine serum albumin, followed by incubation with FITC-trastuzumab (30 μ g) for 1 h at 4°C. Then the samples were analyzed using an LSR-II flow cytometer (Becton Dickinson). The HER2-targeting capability of the H6F peptide was investigated using the same protocols. Instead of FITC-trastuzumab, FITC-H6F (50 μ mol/L, 200 μ L) was used in cell staining, and 15 μ g of FITC-H6F were applied in the flow cytometry experiment.

Binding Affinity of HYNIC-H6F to HER2

The receptor-binding affinity of HYNIC-H6F was assessed in vitro (24). For binding assays, HYNIC-¹²⁵I-H6F was prepared in high specific

activity (44.4 MBq/nmol). The in vitro HER2-binding affinity/specificity of HYNIC-H6F was compared with that of H6F and trastuzumab. HER2-positive MDA-MB-453 cells were incubated with 200,000 cpm of HYNIC-¹²⁵I-H6F and various concentrations of competitive inhibitors for 2 h at 4°C. The cells were then washed with ice-cold 0.1 M phosphate-buffered saline (pH 7.4) to remove free radioactivity. The cells with bound radioactivity were collected, and the radioactivity was measured in a γ -counter (Wallac 1470-002; Perkin Elmer). The results were expressed as the percentage of the bound radioactivity versus total added radioactivity after decay correction. All experiments were performed twice with 4 samples for each.

Small-Animal SPECT/CT Imaging

A small-animal SPECT/CT imaging study was performed on mice bearing MDA-MB-453 or MDA-MB-231 breast cancer xenografts. Each tumor-bearing mouse was injected via the tail vein with 37 MBq of ^{99m}Tc-HYNIC-H6F (4 per group). The blocking study was also performed on MDA-MB-453 mice (4 per group) by coinjection of 37 MBq of ^{99m}Tc-HYNIC-H6F with an excess dose of the H6F peptide (200 μ g) or trastuzumab (500 μ g). At 30 min, 1 h, and 2 h after injection, the mice were anesthetized by inhalation of 2% isoflurane and imaged using nanoScan (Mediso Inc.) following a standard protocol. The pinhole SPECT images (peak, 140 keV; 20% width; frame time, 25 s) were acquired for 13.5 min, and CT images were subsequently acquired (50 kVp; 0.67 mA; rotation, 210°; exposure time, 300 ms). All SPECT images were reconstructed and further analyzed with Fusion (Mediso Ltd.) by drawing volumes of interest on tumor and major organs such as liver (without gallbladder), heart, and kidneys.

Biodistribution

Female mice bearing MDA-MB-453 or MDA-MB-231 tumor xenografts were injected with 0.37 MBq of ^{99m}Tc-HYNIC-H6F to evaluate the distribution of ^{99m}Tc-HYNIC-H6F in tumors and major organs (4 per group). The mice were sacrificed and dissected at 30 min, 1 h, and 2 h after injection. Blood, tumor, liver (without gallbladder), and other major organs were collected and weighed. The radioactivity in the tissue was measured using a γ -counter. The results are presented as the percentage injected dose per gram of tissue (%ID/g). Blocking studies were also performed on 4 mice bearing MDA-MB-453 tumors. For the H6F peptide-blocking group, each mouse was coinjected with 200 μ g of unlabeled H6F peptide and 0.37 MBq of ^{99m}Tc-HYNIC-H6F. At 30 min after injection, all mice in the blocking group were sacrificed, and the organ biodistribution of ^{99m}Tc-HYNIC-H6F was determined.

Statistical Analysis

Quantitative data are expressed as the mean \pm SD. Statistical analysis of image quantification and biodistribution was performed with one-way ANOVA and the Student *t* test with Prism 5.0 (GraphPad Software, Inc.). A *P* value of less than 0.05 was considered statistically significant. The best-fit 50% inhibitory concentrations were calculated by fitting the data with nonlinear regression one-site competitive binding using Prism 5.0.

RESULTS

Chemistry and Radiochemistry

HYNIC-H6F was obtained in 68% yield with a retention time of 14.8 min using analytic HPLC. Matrix-assisted laser desorption/ionization time-of-flight mass spectrometry detected 1,423.41 (m/z) (C₇₁H₈₆N₁₄O₁₆S; calculated molecular weight, 1,423.61). The product was confirmed by mass spectroscopy analysis (Supplemental Fig. 1A; supplemental materials are available at <http://jnm.snmjournals.org>). The HPLC purity of HYNIC-H6F was greater than 95%, and thus, HYNIC-H6F was directly used for a receptor-binding

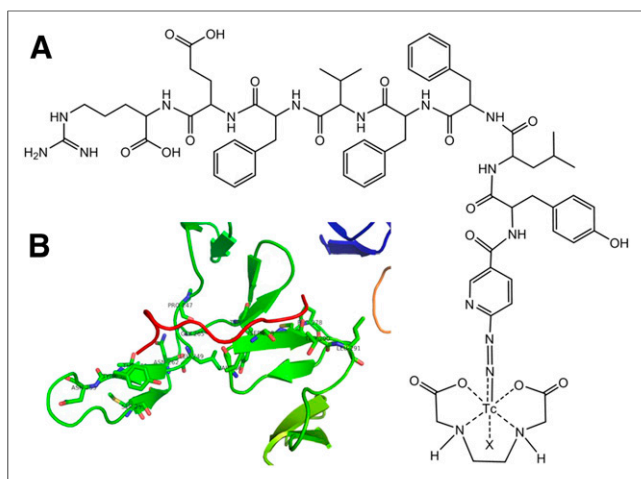


FIGURE 1. (A) Structure of ^{99m}Tc -HYNIC-H6F. (B) Active site structure of complex of HER2 (green lines) with H6F (red line).

assay and ^{99m}Tc radiolabeling. The ^{99m}Tc -labeling procedure was performed within 25 min, with a labeling yield of 92.6%. After purification, the radiochemical purity of ^{99m}Tc -HYNIC-H6F was greater than 95% as determined by radio-HPLC (Supplemental Fig. 1B), and the specific activity of ^{99m}Tc -HYNIC-H6F was more than 35 MBq/nmol. The structure of ^{99m}Tc -HYNIC-H6F is

shown in Figure 1A, and the analysis of the H6F peptide with HER2 using AutoDock (25) is shown in Figure 1B.

Fluorescence Staining and Flow Cytometry

The HER2-targeting capability of the H6F peptide was evaluated in MDA-MB-453 and MDA-MB-231 cells in vitro. The results of incubation with FITC-trastuzumab clearly demonstrated that MDA-MB-453 cells were HER2-positive whereas MDA-MB-231 cells were HER2-negative (Figs. 2A and 2B), consistent with the results of previous studies (26,27). The FITC-labeled H6F peptide exhibited similar binding specificity with trastuzumab in selected breast cancer cells (Fig. 2A). Double fluorescent staining revealed that both Cy3-trastuzumab and FITC-H6F accumulated on the cell membrane in MDA-MB-453 cells (Supplemental Fig. 2).

SPECT/CT Imaging with

^{99m}Tc -HYNIC-H6F

Tumor imaging using ^{99m}Tc -HYNIC-H6F was evaluated in mice bearing MDA-MB-453 and MDA-MB-231 tumors. SPECT images were acquired at 30 min, 1 h, and 2 h after the administration of ^{99m}Tc -HYNIC-H6F. HER2-positive tumors were detected as early as 30 min after injection with high contrast compared with the contralateral background (Fig. 3A). The biodistribution patterns of ^{99m}Tc -HYNIC-H6F in normal organs were similar in both mouse groups (Figs. 3A–3C). Uptake of ^{99m}Tc -HYNIC-H6F was high in the gallbladder in both groups because of its high lipophilicity. However, uptake of ^{99m}Tc -HYNIC-H6F was significantly higher in MDA-MB-453 tumors than in MDA-MB-231 tumors (Fig. 3C), and orthotopic MDA-MB-453 tumors were clearly visualized by SPECT/CT imaging (Supplemental Fig. 3).

H6F and Trastuzumab

Blocking Studies

Unlabeled H6F peptides were coinjected with ^{99m}Tc -HYNIC-H6F to assess the binding specificity in MDA-MB-453 tumors, and images and quantification results clearly demonstrated that the radioactive signals of the imaging tracer were mostly blocked (Figs. 4A and 4B). However, MDA-MB-453 tumors were still clearly visible in the trastuzumab blocking group, indicating that ^{99m}Tc -HYNIC-H6F can be used to detect HER2-positive tumors during trastuzumab-based therapy without concern about the competitive binding of trastuzumab. The HER2-binding affinity of HYNIC-H6F to HER2-positive MDA-MB-453 cells was compared with that of H6F using a competition binding assay with HYNIC- ^{125}I -H6F as a radioligand (Fig. 4C). The 50% inhibitory concentrations for HYNIC-H6F and H6F were 11.25 ± 2.14 and 7.48 ± 3.26 nM, respectively, confirming that the conjugation of HYNIC had little impact on ligand–receptor binding affinity. Furthermore, excess unlabeled HYNIC-H6F significantly inhibited the binding of HYNIC- ^{125}I -H6F to the HER2 protein (Supplemental Fig. 4). However,

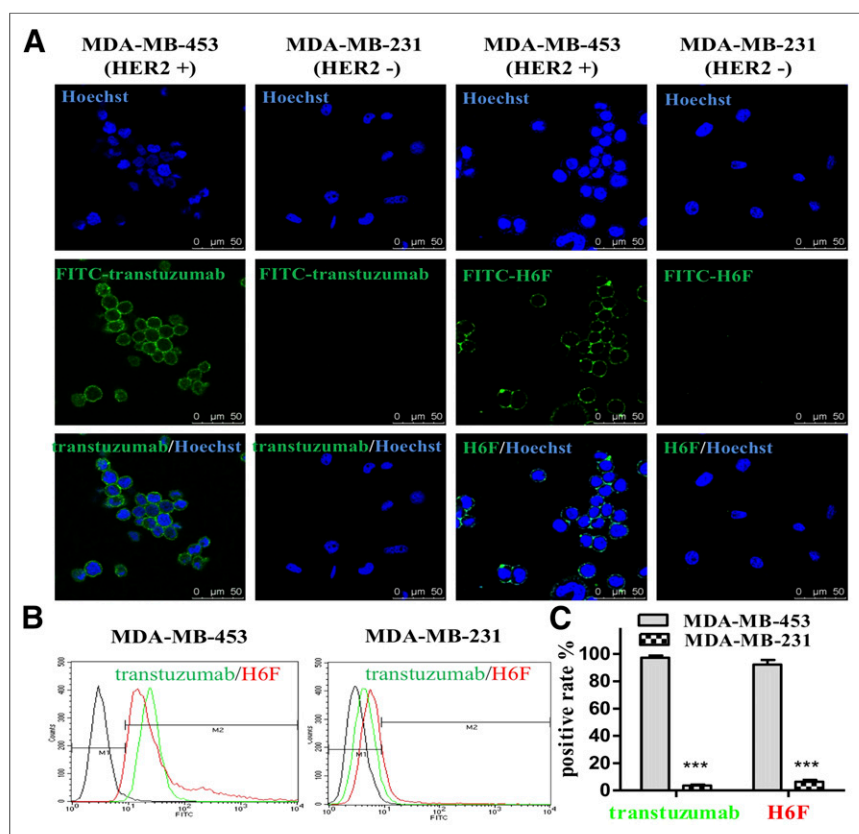


FIGURE 2. (A) Staining of MDA-MB-453 (HER2-positive) and MDA-MB-231 (HER2-negative) cells with FITC-trastuzumab and FITC-H6F. (B) Representative flow cytometry histograms of MDA-MB-453 and MDA-MB-231 cells without ligand (blackout spectrum). (C) Comparison of binding rates of FITC-trastuzumab and FITC-H6F to MDA-MB-453 and MDA-MB-231 cells.

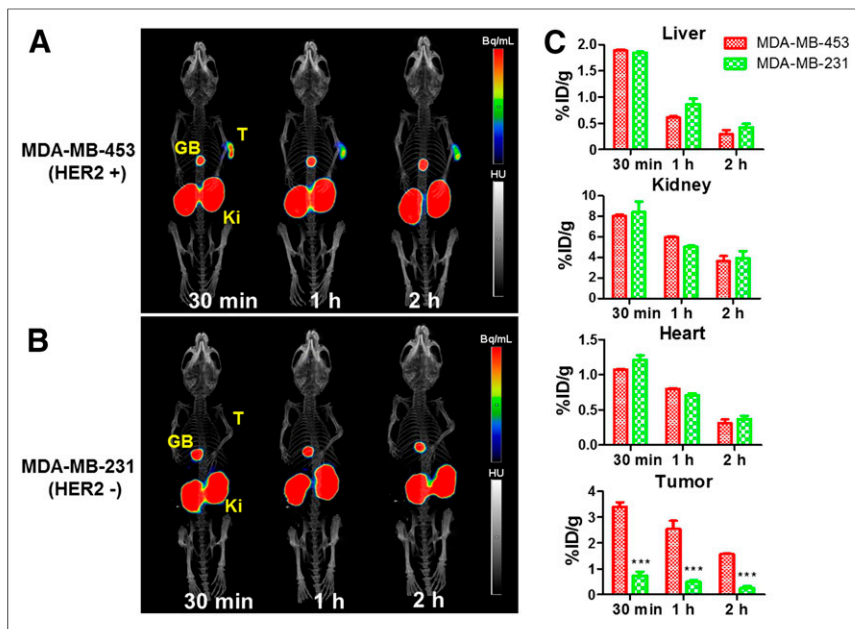


FIGURE 3. (A and B) Representative SPECT/CT images obtained at 30 min, 1 h, and 2 h after injection of ^{99m}Tc -HYNIC-H6F in MDA-MB-453 (A) and MDA-MB-231 (B) tumor-bearing mice. (C) Quantification of liver, kidney, heart, and tumor uptake from A and B. *** $P < 0.001$. GB = gallbladder; Ki = kidney; T = tumor.

trastuzumab did not inhibit the binding of HYNIC- ^{125}I -H6F in vitro (Fig. 4C).

Biodistribution

The biodistribution results for ^{99m}Tc -HYNIC-H6F at 30 min, 1 h, and 2 h after injection are summarized in Figure 5. Uptake of ^{99m}Tc -HYNIC-H6F in MDA-MB-453 tumors was 2.47 ± 0.12 , 0.66 ± 0.24 , and 0.21 ± 0.05 %ID/g at 30 min, 1 h, and 2 h, respectively, after injection (Fig. 5A). Uptake of ^{99m}Tc -HYNIC-H6F was significantly higher in tumors than in normal organs such as the heart, spleen, intestine, and muscle at nearly all time points examined.

The biodistribution patterns of ^{99m}Tc -HYNIC-H6F in normal organs, except liver, were similar between HER2-negative

drugs have been designed to improve outcomes for millions of breast cancer patients. Trastuzumab alone or in combination with other chemotherapy drugs is approved for first-line treatment of HER2-positive breast cancer. However, the trastuzumab monotherapy response rate for metastatic breast cancer is less than 34% (29,30). Real-time monitoring of therapeutic response in breast cancer patients is clinically important if the therapy is to be used as an individualized tool in precision medicine.

In this study, a HER2-targeting peptide, H6F, was modified with a bifunctional chelator and then labeled with ^{99m}Tc to form a novel SPECT imaging agent, ^{99m}Tc -HYNIC-H6F. ^{99m}Tc is one of the most commonly used radionuclides in the clinic, and its appropriate half-life and excellent radiochemical properties make it

suitable for peptide-based nuclear imaging. Tricine/trisodium triphenylphosphine-3,3',3''-trisulfonate was used as a coligand and reductant in the radiolabeling protocol. The whole procedure was rapid and efficient, with a high labeling yield, consistent with the convenient formulation of a labeling kit (31). Moreover, ^{99m}Tc -HYNIC-H6F exhibited excellent in vitro stability in saline for 6 h (Supplemental Fig. 5). In both cell-staining and flow cytometry studies, FITC-H6F exhibited tumor cell-binding features but a lower affinity for receptors than FITC-trastuzumab. In HER2-positive SKBR3 breast cells, there is a significant decrease in FITC-H6F fluorescence signals on transfection of the recombinant plasmid pRNAi-HER2 in HER2-positive SKBR3 breast cells, confirming that the HER2 protein is the specific target of the H6F peptide (22). Furthermore, the introduction

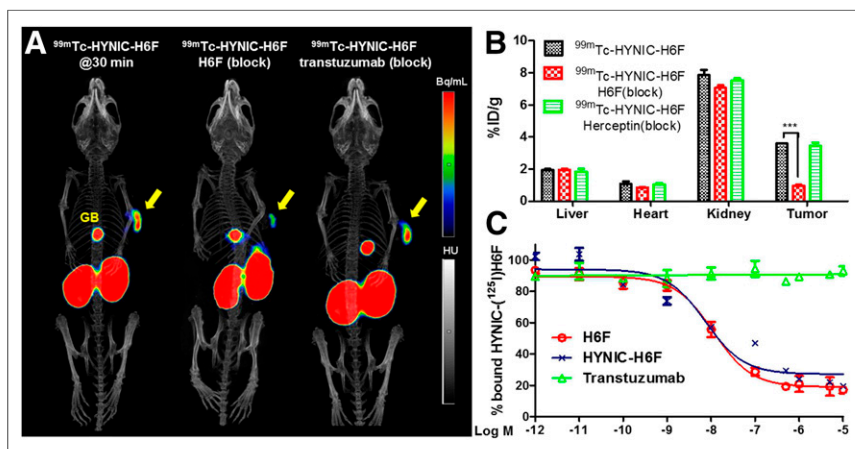


FIGURE 4. (A) Representative SPECT/CT images obtained at 30 min after injection of ^{99m}Tc -HYNIC-H6F in MDA-MB-453 tumor-bearing mice with or without blocking doses of cold H6F peptide or trastuzumab. (B) Quantification of SPECT imaging results. (C) Inhibition of HYNIC- ^{125}I -H6F binding to HER2 on MDA-MB-453 cells by H6F, HYNIC-H6F, and trastuzumab. Arrows indicate tumors.

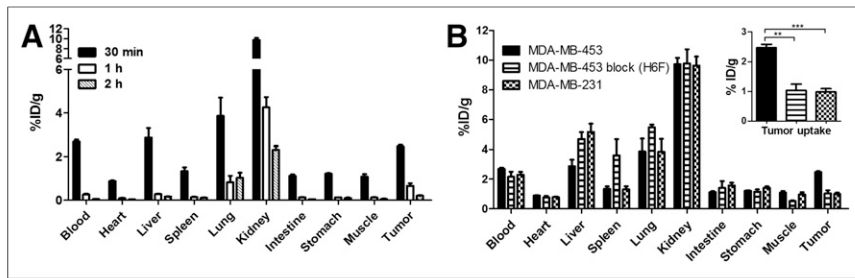


FIGURE 5. (A) Biodistribution of ^{99m}Tc-HYNIC-H6F in MDA-MB-453 tumor-bearing mice at 30 min, 1 h, and 2 h after injection. (B) Biodistribution of ^{99m}Tc-HYNIC-H6F in MDA-MB-453 and MDA-MB-231 tumor-bearing mice at 30 min after injection and in MDA-MB-453 tumor-bearing mice coinjected with cold H6F peptide as blocking agent at 30 min after injection. Inset: ^{99m}Tc-HYNIC-H6F tumor uptake values from B. ***P* < 0.01. ****P* < 0.001.

of HYNIC to the original H6F peptide did not significantly affect its binding affinity to the HER2 protein (Fig. 4C). The easy labeling protocol, favorable stability, high specificity, and good receptor-binding affinity support further application to tumor imaging in animal models.

SPECT/CT imaging and the biodistribution in mice injected with ^{99m}Tc-HYNIC-H6F revealed rapid accumulation and relatively high uptake in subcutaneous HER2-positive MDA-MB-453 tumors and very low uptake in HER2-negative MDA-MB-231 tumors. The maximum uptake values of the radiotracer were observed at 30 min after injection, and the highest tumor-to-organ ratios were observed at 1 h after injection. The rapid clearance from normal organs reduces the wait time between administration and imaging and avoids an unnecessary radiation dose burden to surrounding tissues. In addition, SPECT imaging with ^{99m}Tc-HYNIC-H6F accurately located small orthotopic tumors (<5 mm in diameter) in the right mammary fat pads of female mice (Supplemental Fig. 3), indicating potential clinical applications of ^{99m}Tc-HYNIC-H6F in whole-body screening of HER2-positive metastatic tumors. Coinjection of excess unlabeled H6F peptide effectively blocked uptake of ^{99m}Tc-HYNIC-H6F in HER2-positive tumors, confirming that the binding of ^{99m}Tc-HYNIC-H6F with HER2 was receptor-mediated.

Trastuzumab plays its antitumor function in HER2-positive breast cancers by partially relying on the activation of antibody-dependent cellular cytotoxicity and increased intracellular degradation of HER2 via binding (32,33), which can induce the loss of HER2-positive cells and downregulation of HER2 expression in tumors. Moreover, HER2-positive breast cancer tumors converted to HER2-negative in about one third of patients during trastuzumab-based neoadjuvant therapy (34). Monitoring HER2 expression without trastuzumab blocking during therapy is important for determining the following treatment strategy. Ligand binding site analyses demonstrated that H6F targeted domain II of the extracellular segment of HER2, whereas trastuzumab bound HER2 in the C-terminal portion of domain IV (35,36). The binding of different domains of HER2 by the H6F peptide and trastuzumab permits real-time monitoring of HER2 expression with H6F-based imaging tracers during trastuzumab-based monotherapy and combined therapy. Radioligand competition binding assays demonstrated that excess trastuzumab did not block the binding of radiolabeled H6F to HER2 in HER2-positive MDA-MB-435 cells (Fig. 4C). Similarly, coinjection with trastuzumab did not inhibit the tumor accumulation of ^{99m}Tc-HYNIC-H6F (Fig. 4A). Thus, ^{99m}Tc-HYNIC-H6F recognizes HER2 on tumor cells and does not compete with

trastuzumab for binding during therapy. Different tumor subtypes vary widely in sensitivity to trastuzumab inhibition, partly because of differences in HER2 expression and downregulation levels during therapeutic courses. Imaging with ^{99m}Tc-HYNIC-H6F can supply real-time feedback on HER2 status and guide the adjustment of treatment strategies.

In the last decade, several HER2-targeted peptides have been identified and evaluated for applications in tumor inhibition or drug delivery (37–40), and some specific agents have been used in NIRF imaging (41,42). However, little research on peptide-based nuclear imaging of HER2 has been reported. In this study, we developed ^{99m}Tc-HYNIC-H6F as a SPECT radiotracer for noninvasive imaging of HER2 expression in vivo. SPECT/CT with ^{99m}Tc-HYNIC-H6F could effectively detect HER2-positive breast cancers with high tumor-to-muscle ratios. Because of differences between the targeted domains of ^{99m}Tc-HYNIC-H6F and trastuzumab, ^{99m}Tc-HYNIC-H6F imaging not only can facilitate selection of patients for HER2-targeted therapy but also effectively monitors the therapeutic efficacy of trastuzumab by rechecking the expression level of HER2 without blocking effect during therapy.

CONCLUSION

The ^{99m}Tc-HYNIC-H6F peptide probe specifically accumulates in HER2-positive tumors and is therefore promising for the diagnosis of HER2-positive cancers. Because ^{99m}Tc-HYNIC-H6F and trastuzumab target different regions of the HER2 receptor, this radiotracer also has great potential for monitoring the therapeutic efficacy of trastuzumab by rechecking the expression level of HER2 without blocking effect during therapy.

DISCLOSURE

This research was supported by National Natural Science Foundation of China (NSFC) projects (81630045, 81420108019, 81125011, 81321003, 81427802), a grant from the Beijing Ministry of Science and Technology (Z14110000214004), and the Strategic Priority Research Program of the Chinese Academy of Sciences (XDA12020216). No other potential conflict of interest relevant to this article was reported.

ACKNOWLEDGMENT

Chengyan Dong and Fan Wang contributed equally to this work. They designed this project and revised the manuscript together.

REFERENCES

1. Siegel RL, Miller KD, Jemal A. Cancer statistics, 2015. *CA Cancer J Clin.* 2015;65:5–29.
2. Roder D, Houssami N, Farshid G, et al. Population screening and intensity of screening are associated with reduced breast cancer mortality: evidence of efficacy of mammography screening in Australia. *Breast Cancer Res Treat.* 2008;108:409–416.
3. La Vecchia C, Bosetti C, Lucchini F, et al. Cancer mortality in Europe, 2000–2004, and an overview of trends since 1975. *Ann Oncol.* 2010;21:1323–1360.
4. Berry DA, Cronin KA, Plevritis SK, et al. Effect of screening and adjuvant therapy on mortality from breast cancer. *N Engl J Med.* 2005;353:1784–1792.

5. Tai W, Mahato R, Cheng K. The role of HER2 in cancer therapy and targeted drug delivery. *J Control Release*. 2010;146:264–275.
6. Puglisi F, Fontanella C, Amoroso V, et al. Current challenges in HER2-positive breast cancer. *Crit Rev Oncol Hematol*. 2016;98:211–221.
7. Ahmed S, Sami A, Xiang J. HER2-directed therapy: current treatment options for HER2-positive breast cancer. *Breast Cancer*. 2015;22:101–116.
8. Slamon DJ, Clark GM, Wong SG, Levin WJ, Ullrich A, McGuire WL. Human breast cancer: correlation of relapse and survival with amplification of the HER-2/neu oncogene. *Science*. 1987;235:177–182.
9. Figueroa-Magalhães MC, Jelovac D, Connolly RM, Wolff AC. Treatment of HER2-positive breast cancer. *Breast*. 2014;23:128–136.
10. Pinto AC, Ades F, de Azambuja E, Piccart-Gebhart M. Trastuzumab for patients with HER2 positive breast cancer: delivery, duration and combination therapies. *Breast*. 2013;22(suppl 2):S152–S155.
11. Rimawi MF, Schiff R, Osborne CK. Targeting HER2 for the treatment of breast cancer. *Annu Rev Med*. 2015;66:111–128.
12. Schramm A, De Gregorio N, Widschwendter P, Fink V, Huober J. Targeted therapies in HER2-positive breast cancer: a systematic review. *Breast Care (Basel)*. 2015;10:173–178.
13. Marusyk A, Polyak K. Tumor heterogeneity: causes and consequences. *Biochim Biophys Acta*. 2010;1805:105–117.
14. Capala J, Bouchelouche K. Molecular imaging of HER2-positive breast cancer: a step toward an individualized ‘image and treat’ strategy. *Curr Opin Oncol*. 2010;22:559–566.
15. Gebhart G, Flamen P, De Vries EG, Jhaveri K, Wimana Z. Imaging diagnostic and therapeutic targets: human epidermal growth factor receptor 2. *J Nucl Med*. 2016;57(suppl 1):81S–88S.
16. Cai W, Niu G, Chen X. Multimodality imaging of the HER-kinase axis in cancer. *Eur J Nucl Med Mol Imaging*. 2008;35:186–208.
17. Corcoran EB, Hanson RN. Imaging EGFR and HER2 by PET and SPECT: a review. *Med Res Rev*. 2014;34:596–643.
18. Niu G, Cai W, Chen X. Molecular imaging of human epidermal growth factor receptor 2 (HER-2) expression. *Front Biosci*. 2008;13:790–805.
19. Lee S, Xie J, Chen X. Peptides and peptide hormones for molecular imaging and disease diagnosis. *Chem Rev*. 2010;110:3087–3111.
20. Deutscher SL. Phage display in molecular imaging and diagnosis of cancer. *Chem Rev*. 2010;110:3196–3211.
21. Reubi JC, Maecke HR. Peptide-based probes for cancer imaging. *J Nucl Med*. 2008;49:1735–1738.
22. Wang Z, Wang W, Bu X, et al. Microarray based screening of peptide nano probes for HER2 positive tumor. *Anal Chem*. 2015;87:8367–8372.
23. Dong C, Yang S, Shi J, et al. SPECT/NIRF dual modality imaging for detection of intraperitoneal colon tumor with an avidin/biotin pretargeting system. *Sci Rep*. 2016;6:18905.
24. Dong C, Zhao H, Yang S, et al. ^{99m}Tc-labeled dimeric octreotide peptide: a radiotracer with high tumor uptake for single-photon emission computed tomography imaging of somatostatin receptor subtype 2-positive tumors. *Mol Pharm*. 2013;10:2925–2933.
25. Morris GM, Huey R, Lindstrom W, et al. AutoDock4 and AutoDockTools4: automated docking with selective receptor flexibility. *J Comput Chem*. 2009;30:2785–2791.
26. Kulhari H, Pooja D, Shrivastava S, et al. Trastuzumab-grafted PAMAM dendrimers for the selective delivery of anticancer drugs to HER2-positive breast cancer. *Sci Rep*. 2016;6:23179.
27. Rusnak DW, Alligood KJ, Mullin RJ, et al. Assessment of epidermal growth factor receptor (EGFR, ErbB1) and HER2 (ErbB2) protein expression levels and response to lapatinib (Tykerb, GW572016) in an expanded panel of human normal and tumour cell lines. *Cell Prolif*. 2007;40:580–594.
28. Brown-Glaberman U, Dayao Z, Royce M. HER2-targeted therapy for early-stage breast cancer: a comprehensive review. *Oncology (Williston Park)*. 2014;28:281–289.
29. Nahta R, Esteva FJ. Trastuzumab: triumphs and tribulations. *Oncogene*. 2007;26:3637–3643.
30. Fujita T, Doihara H, Kawasaki K, et al. PTEN activity could be a predictive marker of trastuzumab efficacy in the treatment of ErbB2-overexpressing breast cancer. *Br J Cancer*. 2006;94:247–252.
31. Liu S, Kim YS, Hsieh WY, Gupta Sreerama S. Coligand effects on the solution stability, biodistribution and metabolism of the ^{99m}Tc-labeled cyclic RGDfK tetramer. *Nucl Med Biol*. 2008;35:111–121.
32. Chung A, Cui X, Audeh W, Giuliano A. Current status of anti-human epidermal growth factor receptor 2 therapies: predicting and overcoming Herceptin resistance. *Clin Breast Cancer*. 2013;13:223–232.
33. Hurwitz E, Stancovski I, Sela M, Yarden Y. Suppression and promotion of tumor growth by monoclonal antibodies to ErbB-2 differentially correlate with cellular uptake. *Proc Natl Acad Sci USA*. 1995;92:3353–3357.
34. Mittendorf EA, Wu Y, Scaltriti M, et al. Loss of HER2 amplification following trastuzumab-based neoadjuvant systemic therapy and survival outcomes. *Clin Cancer Res*. 2009;15:7381–7388.
35. Bussolati G, Montemurro F, Righi L, Donadio M, Aglietta M, Sapino A. A modified Trastuzumab antibody for the immunohistochemical detection of HER-2 overexpression in breast cancer. *Br J Cancer*. 2005;92:1261–1267.
36. Cho HS, Mason K, Ramyar KX, et al. Structure of the extracellular region of HER2 alone and in complex with the Herceptin Fab. *Nature*. 2003;421:756–760.
37. Geng L, Wang Z, Yang X, et al. Structure-based design of peptides with high affinity and specificity to HER2 positive tumors. *Theranostics*. 2015;5:1154–1165.
38. Nakajima H, Mizuta N, Sakaguchi K, et al. Development of HER2-antagonistic peptides as novel anti-breast cancer drugs by in silico methods. *Breast Cancer*. 2008;15:65–72.
39. Tan M, Lan KH, Yao J, et al. Selective inhibition of ErbB2-overexpressing breast cancer in vivo by a novel TAT-based ErbB2-targeting signal transducers and activators of transcription 3-blocking peptide. *Cancer Res*. 2006;66:3764–3772.
40. Wang XF, Birringer M, Dong LF, et al. A peptide conjugate of vitamin E succinate targets breast cancer cells with high ErbB2 expression. *Cancer Res*. 2007;67:3337–3344.
41. Joshi BP, Zhou J, Pant A, et al. Design and synthesis of near-infrared peptide for in vivo molecular imaging of HER2. *Bioconjug Chem*. 2016;27:481–494.
42. Geng L, Wang Z, Jia X, et al. HER2 targeting peptides screening and applications in tumor imaging and drug delivery. *Theranostics*. 2016;6:1261–1273.